

Transient Electronic Transport Properties through a Quantum Dots Ring

W. A. Abdul-Hussein

Department of science, College of basic education, Sumer university, Thi-Qar, Iraq

*Corresponding author E-mail: wisam122@yahoo.com

Abstract

In this paper a theoretical study of the effect of the electron transport in a quantum dot ring, which is consisted from four quantum dots, connected with two electrode metal. For this purpose, a single-electron model was used in this system. The Hamiltonian of this system is consisted from a single level for each quantum dots. The influence of energy levels of the electrode metal was taken into consideration. The Time-dependent equations of motion were found using the Laplace transform, which was enabled the occupation-probability to be found for the right electrode. Results shown that the occupation-probability and the current flowing exhibit oscillations in the elementary stage of the transport process and finally progress into stationary values. So, the occupation probability of the R-electrode increased with the coupling interaction of the QDs and the bias voltage, but it is reduced by increasing the electrodes-QDs interaction and absolute temperature.

Keywords: Electron Transport, Quantum Dots, Ring Structure.

1. Introduction

The electron transport process (ET) through a quantum dot (QD) system has been investigated in many fields, theoretical and experimental, as physical, Chemical and Biological[1-4]. In recent years, there have been new Developments in the study of electron transport process, especially after the increase in the application of modern methods during the study of the transport of electrons in chemical and biological systems [5,6]. It is possible to examine the interaction of electron transfer entirely through the methods of quantum chemistry. These studies used complex computer programs and fast computers, which aim to understand the ways in which the probability of ET depends on the characteristics of each of the components of the system, and the parameters involved in this process, as electronic coupling between quantitative cases that have a qualitative impact [7].

In this paper, we design a kind of four quantum dots (QDs) are circularly coupled setup, a ring shaped, connected with two electron electrodes to investigate the transient ET properties, as shown in figure 1.

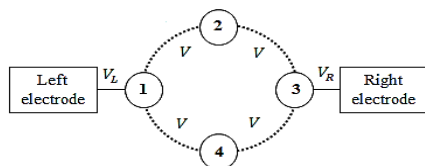


Fig 1: Schematic diagrams of quantum dot ring connected with two electrodes.

The electrodes are described as sources or electrodes of electrons that have a corresponding energy level in which the number of electrons is changing, and they are connected to the source of the

bias voltage. The probability of electronic distribution in these electrodes follows the Fermi distribution function [8-10],

$$f(E, \mu) = \frac{1}{e^{\frac{E-\mu}{k_B T}} + 1}$$

where k_B , T , E , and μ are Boltzmann's constant, the absolute temperature, the energy of the single-electron in the electrode, and the total chemical potential, respectively. At zero temperature without bias voltage ($V_{bias} = 0$), the chemical potential is equal to the Fermi energy (which is in an equilibrium state), and the energy levels are filled up to the Fermi-level, and the Fermi distribution function is equal to one at $E < \mu$ or zero at $E > \mu$. While applying a bias voltage on the right electrode, the chemical potentials will be different according to $\mu_L - \mu_R = eV_{bias}$ and $\mu_R = \epsilon_f - eV_{bias}$ [11], which lead to the flow of electrons from the left to the right electrode.

2. Model and Formulae

A quantum dot ring is consisted from four quantum dots, which connected with two electrodes by tunnel coupling, as showing in figure 1, the Hamiltonian of the system, as a tight-binding model, can be written as

$$H = H_\alpha + H_D + H_{\alpha D} + H_{DD} \quad (1)$$

Here, $H_\alpha (H_D)$ is represent the isolated electrode (dot) Hamiltonian, $H_\alpha = \sum_{jL} E_{jL} P_{jL}(t) + \sum_{jR} E_{jR} P_{jR}(t)$ ($H_D = \sum_{k=1}^4 \epsilon_k D_k^\dagger D_k$), where $P_{j\alpha}(t) = a_{j\alpha}^\dagger a_{j\alpha}$, and $a_{j\alpha}^\dagger |a_{j\alpha}$ are the creation [annihilation] operators of the electrons in the left ($\alpha = L$) or right ($\alpha = R$) electrode with j wave vector; $E_{jL} |E_{jR}$ are the energies of the single electron in the L and R electrode, respectively. $D_k^\dagger |D_k (\epsilon_k)$ are the creation [annihilation] operators (energy level) of the k -th quantum dot. $H_{\alpha D} (H_{DD})$ describes the coupling between electrodes and quantum dots (quantum dots and

quantum dots), $H_{\alpha D} = \sum_j V_{jL} a_{jL}^+ D_1 + \sum_j V_{jR} a_{jR}^+ D_3 + h.c.$ ($H_{DD} = \sum_{k=1}^4 V D_k^+ D_k + h.c.$), with $V_{jL}|V_{jR}$ (V) are the coupling interaction between the $L|R$ electrode and the $1|3$ dot (k th and the $(k+1)$ th D , at $k=4, i+1 \rightarrow 1$). The equations of motion for this system can be obtained by using [12],

$$\dot{D}_k = -\frac{i}{\hbar} \frac{dH}{dD_k^+}(t)$$

with ($e = \hbar = 1$ a.u.) i.e.

$$\left. \begin{aligned} \dot{D}_1(t) + i\varepsilon_1 D_1(t) + iVD_2(t) + iVD_4(t) + i\sum_{jL} V_L a_{jL} &= 0 \\ \dot{D}_2(t) + i\varepsilon_2 D_2(t) + iVD_1(t) + iVD_3(t) &= 0 \\ \dot{D}_3(t) + i\varepsilon_3 D_3(t) + iVD_2(t) + iVD_4(t) + i\sum_{jR} V_R a_{jR} &= 0 \\ \dot{D}_4(t) + i\varepsilon_4 D_4(t) + iVD_3(t) + iVD_1(t) &= 0 \\ \dot{a}_{jL}(t) + iE_{jL} a_{jL}(t) + iV_L D_1(t) &= 0 \\ \dot{a}_{jR}(t) + iE_{jR} a_{jR}(t) + iV_R D_3(t) &= 0 \end{aligned} \right\} \quad (2)$$

The effect of energy levels in metal electrodes on the quantum dots is the addition of a complex part known as self-energy[13], $\sum_{j\alpha} V_{j\alpha}(E)$, i.e. $E_1 = \varepsilon_1 + \sum_{jL}(E) \rightarrow \varepsilon_1 - i\Delta_{jL1}$ and $E_3 = \varepsilon_3 + \sum_{jR}(E) \rightarrow \varepsilon_3 - i\Delta_{jR3}$; where $\Delta_{jL1} = \pi \bar{\rho}_L |V_L|^2$ ($\Delta_{jR3} = \pi \bar{\rho}_R |V_R|^2$) 1st (3th) level broadening due to its level-electrode level coupling interaction. The above system of equations of motion (2) can be solving by using Laplace transform [14], when $\varepsilon_2 = \varepsilon_4 = 0$, as

$$\left. \begin{aligned} D_1(S) &= \frac{D_1(0)S^2 + \sigma_{11}S + \sigma_{12}}{(S - \lambda_1)(S - \lambda_2)(S - \lambda_3)} \\ D_2(S) &= \frac{D_2(0)S^3 + \sigma_{21}S^2 + \sigma_{22}S + \sigma_{23}}{S(S - \lambda_1)(S - \lambda_2)(S - \lambda_3)} \\ D_3(S) &= \frac{D_3(0)S^2 + \sigma_{31}S + \sigma_{32}}{(S - \lambda_1)(S - \lambda_2)(S - \lambda_3)} \\ D_4(S) &= \frac{D_4(0)S^3 + \sigma_{41}S^2 + \sigma_{42}S + \sigma_{43}}{S(S - \lambda_1)(S - \lambda_2)(S - \lambda_3)} \end{aligned} \right\} \quad (3)$$

Where

$$\begin{aligned} \sigma_{12} &= 2V^2(D_1(0) - D_3(0)) + VE_3(D_2(0) + D_4(0)), \\ \sigma_{21} &= i(E_1 + E_3)D_2(0) - iV(D_1(0) + D_3(0)), \\ \sigma_{22} &= 2V^2(D_2(0) - D_4(0)) + V(E_1 D_3(0) + E_3 D_1(0)) - E_1 E_3 D_2(0), \\ \sigma_{23} &= iV^2(D_2(0) - D_4(0))(E_1 + E_3), \\ \sigma_{31} &= -iV(D_2(0) + D_4(0)) + iE_1 D_3(0), \\ \sigma_{32} &= -2V^2(D_1(0) - D_3(0)) + VE_1(D_2(0) + D_4(0)), \\ \sigma_{41} &= i(E_1 + E_3)D_4(0) - iV(D_1(0) + D_3(0)), \\ \sigma_{42} &= 2V^2(D_4(0) - D_2(0)) + V(E_1 D_3(0) + E_3 D_1(0)) - E_1 E_3 D_4(0), \\ \sigma_{43} &= -iV^2(E_1 + E_3)(D_2(0) - D_4(0)), \end{aligned}$$

$$\begin{aligned} \lambda_1 &= \frac{1}{6}(A_1 + 12\sqrt{A_2})^{1/3} - \frac{6A_3}{(A_1 + 12\sqrt{A_2})^{1/3}} - i\frac{1}{3}(E_1 + E_3), \\ \lambda_{2,3} &= -\frac{1}{12}(A_1 + 12\sqrt{A_2})^{1/3} + \frac{3A_3}{(A_1 + 12\sqrt{A_2})^{1/3}} - i\frac{1}{3}(E_1 + E_3) \\ &\quad E_3 \pm 12i316A_1 + 12A_213 + 6A_3A_1 + 12A_213, \end{aligned}$$

$$\begin{aligned} A_1 &= -72i(E_1 + E_3) \left(V^2 - \frac{1}{9}(E_1^2 + E_3^2) + \frac{5}{18}E_1 E_3 \right), \\ A_2 &= 768V^6 + V^4(156(E_1^2 + E_3^2) - 264E_1 E_3) + 24V^2(E_1 - E_3) \\ &\quad E_3^2 E_1^2 + E_3^2 + 12E_1 E_3 + 3E_1^2 E_3^2 E_1 - E_3^2, \end{aligned}$$

$$\text{and } A_3 = \frac{4}{3}V^2 + \frac{1}{9}(E_1^2 + E_3^2 - E_1 E_3)$$

The set equations (3) above can be solved using an inverse Laplace transform, as

$$\left. \begin{aligned} D_{k=1,3}(t) &= \frac{D_k(0)\lambda_1^2 + \sigma_{k1}\lambda_1 + \sigma_{k2}}{(\lambda_1 - \lambda_2)(\lambda_1 - \lambda_3)} e^{\lambda_1 t} - \frac{D_k(0)\lambda_2^2 + \sigma_{k1}\lambda_2 + \sigma_{k2}}{(\lambda_1 - \lambda_2)(\lambda_2 - \lambda_3)} e^{\lambda_2 t} \\ &\quad + \frac{D_k(0)\lambda_3^2 + \sigma_{k1}\lambda_3 + \sigma_{k2}}{(\lambda_1 - \lambda_3)(\lambda_2 - \lambda_3)} e^{\lambda_3 t} \\ D_{k=2,4}(t) &= \frac{D_k(0)\lambda_1^3 + \sigma_{k1}\lambda_1^2 + \sigma_{k2}\lambda_1 + \sigma_{k3}}{\lambda_1(\lambda_1 - \lambda_2)(\lambda_1 - \lambda_3)} e^{\lambda_1 t} - \frac{D_k(0)\lambda_2^3 + \sigma_{k1}\lambda_2^2 + \sigma_{k2}\lambda_2 + \sigma_{k3}}{\lambda_2(\lambda_1 - \lambda_2)(\lambda_2 - \lambda_3)} e^{\lambda_2 t} \\ &\quad + \frac{D_k(0)\lambda_3^3 + \sigma_{k1}\lambda_3^2 + \sigma_{k2}\lambda_3 + \sigma_{k3}}{\lambda_3(\lambda_1 - \lambda_3)(\lambda_2 - \lambda_3)} e^{\lambda_3 t} - \frac{\sigma_{k3}}{\lambda_1 \lambda_2 \lambda_3} \end{aligned} \right\} \quad (4)$$

The probability of the right electrode can be calculated by using this relations [15], $P_{jR}(t) = \sum_{jR} |V_{jR}|^2 |\bar{a}_{jR}(t)|^2$, V_{jR} related with the electronic density of state of right electrode as; $\rho_R(E) = \sum_{jR} |V_{jR}|^2 \delta(E - E_R)$, where $\delta(E - E_R)$ represent Dirac-Delta function. Since $\int \delta(E - E_R) dE = 1$ [16] and by taking $\rho_R(E)$ its average over the energy, $\bar{\rho}_R = 1/4\beta_R$, with $4\beta_R$ is the band-width of the right electrode then $P_R(t)$ is as follows:

$$P_R(t) = \bar{\rho}_R \int |\bar{a}_{jR}(t)|^2 dE \quad (5)$$

Here, $\bar{a}_{jR}(t)$ it can be obtained using the Green's function [17], as

$$\bar{a}_{jR}(t) = e^{-iE_{jR}t} \left(\bar{a}_{jR}(0) - iV_{jR} \int_0^t D_3(\hat{t}) e^{iE_{jR}\hat{t}} d\hat{t} \right) \quad (6)$$

By introducing $D_3(t)$ from eq.(4) and using the initial conditions, $\bar{a}_{jR}(0) = \sqrt{f(E, \mu_R)}$ we get:

$$\begin{aligned} \bar{a}_{jR}(t) &= e^{-iE_{jR}t} \left(\sqrt{f(E, \mu_R)} - iV_{jR} \left[\frac{(D_3(0)\lambda_1^2 + \sigma_{31}\lambda_1 + \sigma_{32})}{(iE_{jR} + \lambda_1)(\lambda_1 - \lambda_2)(\lambda_1 - \lambda_3)} \right. \right. \\ &\quad \left. \left(e^{(iE_{jR} + \lambda_1)t} - 1 \right) - \frac{(D_3(0)\lambda_2^2 + \sigma_{31}\lambda_2 + \sigma_{32})}{(iE_{jR} + \lambda_2)(\lambda_1 - \lambda_2)(\lambda_2 - \lambda_3)} \right. \\ &\quad \left. \left(e^{(iE_{jR} + \lambda_2)t} - 1 \right) + \frac{(D_3(0)\lambda_3^2 + \sigma_{31}\lambda_3 + \sigma_{32})}{(iE_{jR} + \lambda_3)(\lambda_1 - \lambda_3)(\lambda_2 - \lambda_3)} \right. \\ &\quad \left. \left. \left(e^{(iE_{jR} + \lambda_3)t} - 1 \right) \right] \right) \end{aligned} \quad (7)$$

3. Results and Discussion

In this section, we calculate the time probability of the R-electrode $P_R(t)$ and the current $I_R(t)$ flowing through this system for different values of parameters affecting the system, such as V , V_{α} , V_{bias} , and T . The tunneling between all QDs system was switched-off initially (at $t=0$). The system in the equilibrium state, the occupancies of QDs were given as (1,0,0,0). Figure.2 represented the occupation probability of right electrode versus time, which increased in increasing the QDs coupling interaction (V), while decreased with increasing the interaction between electrodes and QDs $V_{L,R}$.

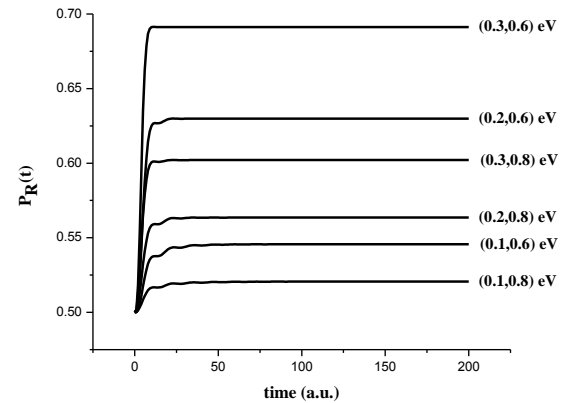


Figure 2: Occupation probability of R electrode versus time for different values of ($V, V_{L,R}$) at $V_{bias} = 0$, and $T = 300$ k.

After a long time ($t=2000$ a.u.), we see that it is enough to be finished the ET, we study the properties of system effects on the

occupation of the R electrode $P_R(t)$. Figure 3 shows the effect of the coupling interaction of the QDs. The $P_R(t)$ is started increasing by increasing the V to reach its maximum value at $V = 0.5$ eV, and then go down when $V > 0.5$ eV to settle at 0.5623444. Also, we observe that increasing the electrodes-QDs interaction ($V_{L,R}$) leads to decrease the $P_R(t)$, as displayed in figure 4.

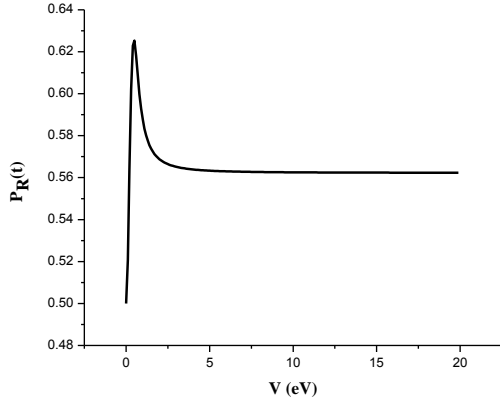


Figure 3: Occupation probability of R electrode versus QDs coupling at $V_{L,R} = 0.8$ eV, $V_{bias} = 0$, and $T = 300$ k.

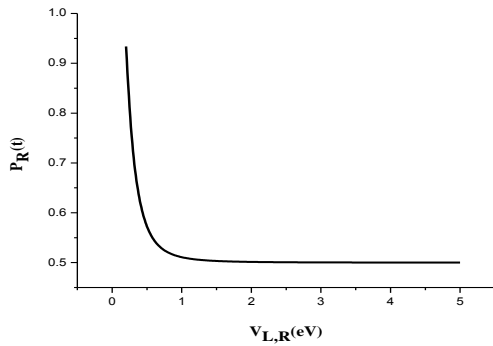


Figure 4: Occupation probability of right electrode versus QDs-electrodes coupling at $V = 0.1$ eV, $V_{bias} = 0$ and $T = 300$ k.

Figures 5 and 6 show the effect of both the bias voltage applied on the right electrode V_{bias} and the absolute temperature T , respectively. We observed that the influence of the V_{bias} leads to linear increase of the $P_R(t)$, while the impact of temperature is very low by 2.396×10^{-4} per 100 k.

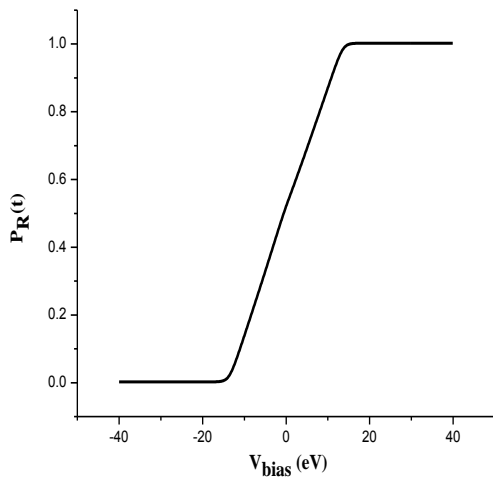


Figure 5: Occupation probability of R electrode versus voltage bias at $V=0.1$, $V_{L,R}=0.8$ eV, $t=2000$ a.u., and $T=300$ k.

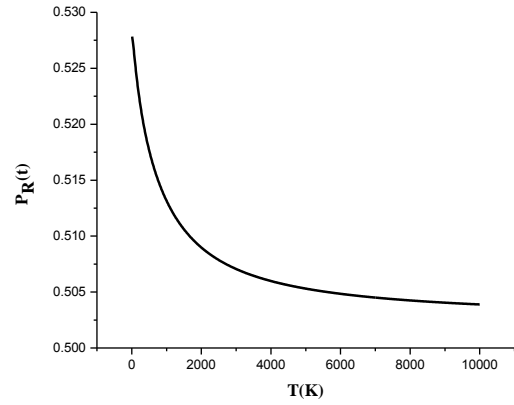


Figure 6: Occupation probability of R electrode versus absolute temperature at $V = 0.1$, $V_{L,R} = 0.8$ eV, and $V_{bias} = 0$.

In this system, the current can be acquired from the evolution of the R-electrode electron occupation number as, $I_R(t) = -e\dot{P}_R(t)$ [18]. In figures 7, 8, and 9, we study the properties of the system effects on the behavior of the current system. By increasing the V QDs to increase the peak of the current (see figure 7), which decreases when the $V_{L,R}$ is increased (see figure 8). While we do not observe any effect of the V_{bias} and T (see figure 9).

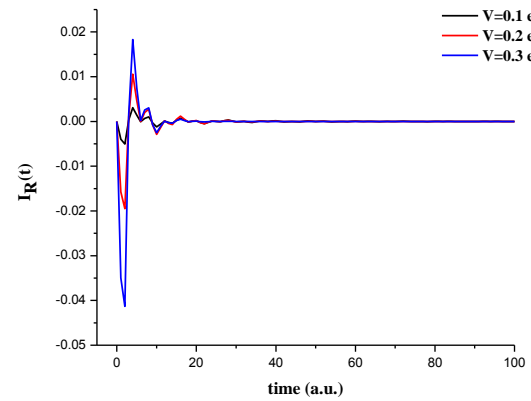


Figure 7: (Color online) Transient-current in the right electrode versus time for different values of V at $V_{L,R} = 0.8$ eV, $V_{bias} = 0$, and $T = 300$ k.

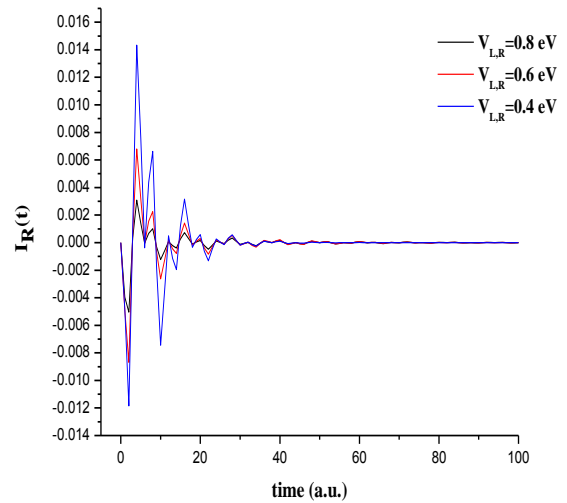


Figure 8: (Color online) Transient-current in the right electrode versus time for different values of $V_{L,R}$ at $V = 0.1$ eV, $V_{bias} = 0$, and $T = 300$ k.

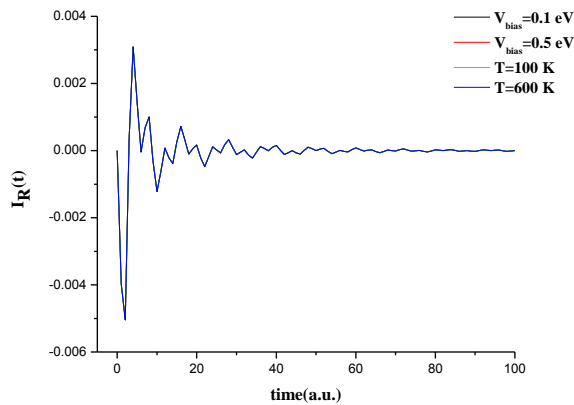


Figure 9: (Color online) Transient-current in the right electrode versus time for different values of V_{bias} , and T at $V = 0.1 eV$, and $V_{L,R} = 0.8 eV$.

4. Conclusions

Firstly, we have derived the equations of motion of the QDs ring connected with L and R-electrodes system, which enabled us to find the occupation probability of R-electrode. Then, the current of the system is shown that the probability of the electrons occupying the R-electrode and the current exhibit transient oscillations in the elementary stage. After that, it became constants eventually. This result indicated that the system has evolved into a stationary-state. Moreover, the occupation probability of the R-electrode increased with the coupling interaction of the QDs and the bias voltage. The same thing is occurred with the peak of the current. While it decreased with increasing the electrodes-QDs interaction and absolute temperature. But, it is not existed in the peak of the current.

References

- [1] D. Sztenkiel, and R. Swirkowicz, Electron Transport through Double Quantum Dots with Interdot Coulomb Repulsion. *ACTA PHYSICA POLONICA A*. 110, 389-394 (2006.)
- [2] W. Li, L. Sepunaru, N. Amdursky, S-R. Cohen, I. Pecht, M. Sheves, and D. Cahen, Temperature and Force Dependence of Nanoscale Electron Transport via the Cu Protein Azurin. *ACS Nano*. 6 (12), 10816–10824 (2012).
- [3] S. Xuan, Z. Meng, X. Wu, J-Ru. Wong, G. Devi, E-K.Lee Yeow, and F. Shao, Efficient DNA-Mediated Electron Transport in Ionic Liquids. *ACS Sustainable Chem. Eng.* 4 (12), 6703–6711 (2016).
- [4] H. Huang, Y. Tan, J. Shi, G. Lianga, and J-Jie Zhu, DNA aptasensor for the detection of ATP based on quantum dots electrochemiluminescence. *Nanoscale*. 2, 606–612 (2010).
- [5] M. A. Shandiz, F. Salvat, and R. Gauvin, Detailed Monte Carlo Simulation of electron transport and electron energy loss spectra. *SCANNING*, 9999, 1-17 (2015).
- [6] B. Weingartner, S. Rotter, and J. Burgdörfer, Simulation of electron transport through a quantum dot with soft walls, *PHYSICAL REVIEW B*, 72, 115342-115351 (2005).
- [7] El Ouchdi, B. Bouazza, Y. Belhadji, and N. Massouma, Study and Simulation of Electron Transport in Ga_{0.5}In_{0.5}Sb Based on Monte Carlo Method. *Semiconductors*. 51(12), 1588–1591 (2017).
- [8] U. Harbola, M. Esposito, and S. Mukamel, Quantum master equation for electron transport through quantum dots and single molecules. *PHYSICAL REVIEW B*. 74, 235309-235322 (2006).
- [9] T. Costi, A. Hewson, and V. Zlatic, Transport coefficients of the Anderson model via the numerical renormalization group. *J. Phys.: Condens. Matter*. 6, 2519-2558 (1994)
- [10] R. Świrkowicz, M. Wierzbicki, and J. Barnaś, Thermoelectric effects in transport through quantum dots attached to ferromagnetic leads with noncollinear magnetic moments. *PHYSICAL REVIEW B*. 80, 195409-195419 (2009).
- [11] L-Hua Yang, C-Lu Yang, M-Shan Wang, and X-Guang Ma, Electronic Transport properties of tetracyclopentadienyl modified with C And Si atoms. *Physics Letters A*. 379, 1726-1731 (2015).
- [12] W. A. Abdul-Hussein, and S. I. Easa. Electron Transport In DBA System Of Multiple Bridges. *Journal of Babylon University/Pure and Applied Sciences*, 21, 1803-1818 (2013).
- [13] S.Tsukamoto, T. Ono, K. Hirose, and S. Blugel, Self-energy matrices for electron transport calculations within the real-space finite-difference formalism. *PHYSICAL REVIEW E* 95, 033309 (2017).
- [14] P. Dyke, *An Introduction to Laplace Transforms and Fourier Series*, 2nd Edition. Springer London. 2014.
- [15] R. Taranko, and T.Kwapiński, 2005. Charge and current beats in T-shaped qubit–detector systems. *Physica E* 70, 217–224 (2015).
- [16] S. Hassani, *Mathematical Methods: For Students of Physics and Related Fields*. Springer New York. (2009).
- [17] K. Watanabe, *Integral Transform Techniques for Green's Function*. Springer International Publishing. (2014).
- [18] Z.T. Jiang, J. Yang, Y. Wang, X. F. Wei, and Q. Z. Han, Transient and stationary transport properties of a three-subring quantum-dot structure. *J. Phys. Condens. Matter*. 20, 445216-445221 (2008).